APEM journal
Advances in Production Engineering & Management
Volume 14 | Number 4 | December 2019 | pp 494–506
https://doi.org/10.14743/apem2019.4.344
ISSN 1854-6250
Journal home: apem-journal.org
Original scientific paper

High-performance end milling of aluminum alloy: Influence of different serrated cutting edge tool shapes on the cutting force

Burek, J.[a], **Plodzien, M.**[a], **Zylka, L.**[a,*], **Sulkowicz, P.**[a]

[a]Department of Manufacturing Techniques and Automation, The Faculty of Mechanical Engineering and Aeronautics, Rzeszow University of Technology, Rzeszow, Poland

ABSTRACT

The article presents the results of experimental studies in high performance milling of AlZn5.5MgCu aluminum alloy. The tests were performed with the use of end mill cutters with different serrated shapes of the cutting edge. End mills with continuous, interrupted and wavy with varied profile radius were used. The tests were conducted on a DMG's DMU 100 MonoBlock machining center with cutting force components measurement in workpiece system capabilities. The experimental tests were carried out using varied radial depth of cut a_e and feed per tooth f_z parameters according to applied three-level full design of experiment. The relationships between a_e and f_z parameters and cutting force components for various cutting edge shapes were determined. A continuous cutting edge was adopted as a reference shape. Based on the results of the tests, cutting force components models for analyzed cutting edge shapes were determined. A comparative analysis between the developed models and relationships was conducted. The study proved that when adopting end mills with serrated cutting edges, lower cutting force components are obtained, in comparison with cutters with continuous cutting edges. The results also showed that for end mills with serrated cutting edges radial depth of cut a_e has a negligible influence on the feed force component F_f. The results proved, that end mills with serrated cutting edges should be used in high performance machining, where high values of a_e and f_z parameters are adopted. Furthermore, machining of thin-walled workpieces can be a potential application of these end mills, as lower values of cutting force components reduce the risk of deformation of milled thin walls.

ARTICLE INFO

Keywords:
High performance milling;
Aluminum alloy (AlZn5.5MgCu);
Cutting force;
Modelling;
End mill cutter;
Serrated cutting edge

**Corresponding author:*
zylka@prz.edu.pl
(Zylka, L.)

Article history:
Received 9 September 2019
Revised 2 December 2019
Accepted 4 December 2019

1. Introduction

Researchers always try to develop new ways to improve milling processes, one of which is to increase cutting parameters, such as cutting depths and widths as well as cutting speed [1-3]. This is mainly the result of constant efforts to reduce machining time and production costs. One of the milling methods, which allows to reduce machining time is high performance cutting (HPC). HPC is used primarily as roughing machining, where high volumes of workpiece material are removed and surface quality is irrelevant. It is difficult to accurately define the concept of high performance machining. Various attempts at defining HPC may be found in the literature. One of the ways to differentiate a high performance cutting from conventional machining is to use a cutting volume Q_w, which depends on the feed rate as well as on the axial and radial depth

of cut [1]. It is commonly accepted, that in HPC the following range of cutting parameters is adopted: a_p is $0.5\,D_c$ to $1.5\,D_c$ (mm), a_e is $0.3\,D_c$ to $1\,D_c$ (mm), f_z is 0.1 to 0.3 (mm/tooth). A characteristic feature of HPC machining is the use of 2-5 times the usual cutting speeds v_c in comparison with conventional machining, in addition to higher feeds per tooth f_z, radial depths of cut a_e and axial depths of cut a_p [4, 5].

One of the practical applications of HPC machining is milling thin-walled integral structures made of aluminum alloys used in aircraft constructions. Such parts are characterized by a large number of closed areas of great depth as well as a high volume of material necessary to be removed and thin-walled structures [5]. As a result, roughing machining has to ensure high milling volumes, but cannot lead to elastic or plastic deformations of milled walls. Thus, it is important to try to reduce the cutting force components, mainly normal to feed cutting force component, and as a result decrease the mechanical load on the milled walls [5-8]. As a result of the local decrease in cutting depth by the value of elastic deformation of the workpiece's wall, additional allowance remains on the workpiece, which has to be cut in the following machining pass. This results in a significant increase in total machining time or leaving larger allowances for finishing machining in order to increase the stiffness of the wall. Therefore, ensuring the proper conditions of HPC machining, that will not result in an occurrence of such cutting force components values, which in turn would cause elastic or plastic deformation of a wall is of great importance [5, 9, 10]. One of the ways to reduce the cutting force components is to use tools with varied cutting edge shape.

For the HPC machining, solid carbide end mill cutters are usually used. In the case of HPC milling of aluminum alloys, 3 flute end mills are commonly used. One of the crucial macrogeometry parameters is cutting edge shape. The cutting edge shape may be continuous, interrupted or wavy, and in the case of the last two, it can also be described as a serrated edge [1, 11]. In the case of interrupted cutting edge, a few different shapes may occur, for example triangular, round, square etc. This type of edge is shaped in the form of notches offset from each other by the constant value. As a result, during the rotation of the cutter, the notches in subsequent edges pass each other. A similar situation takes place in the case of a wavy shape of a cutting edge, which may be shaped with different values of inner and outer radius creating a constant or variable sinusoidal shape [1].

The shape of a cutting edge has a significant impact on the milling process. In particular, it greatly affects the chip forming process, vibrations and cutting forces [11]. In industrial practice, end mills dedicated to roughing machining of aluminum alloys characterized by the varied shape of a cutting edge can be found. There are, however, no experimental tests available, that would clearly indicate what is the effect of the cutting edge shape on the high performance milling of aluminum alloys. The cutting force is a basic process parameter influencing machining and the quality of the workpiece. The determination of the cutting force values during the HPC machining is of significant importance because it allows to determine for example the load on the tool

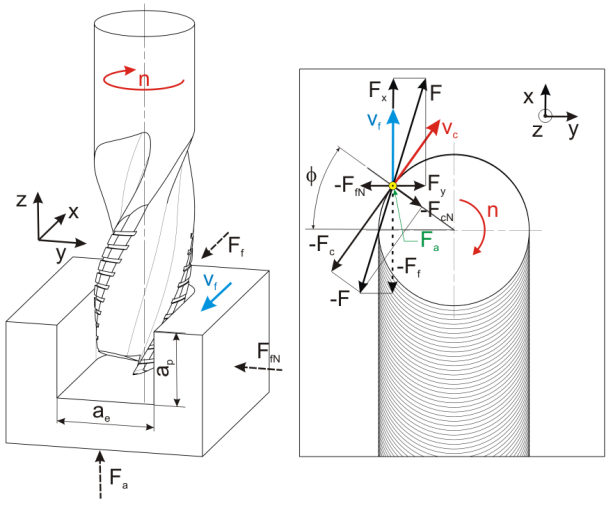

Fig. 1 Cutting forces in end milling

or the load on the thin-walled structures [5]. The total cutting force, which is a sum of vectors of all forces, can be broken into an active force F (in the work plane), and into a reactive force F_a (perpendicular to the work plane), Fig. 1. The active force varies with the cutter contact angle ϕ and may be broken into forces F_f and F_{fN} related to the workpiece, acting in the feed direction, or rotating forces F_c and F_{cN} related to the tool, acting in the cutting speed direction.

Previous works focused mainly on modelling of milling process [12-16]. For instance, Liu *et al*. presented a theoretical model of dynamic cutting force [17]. The influence of the effective rake angle and the size effect of undeformed chip thickness were included in the formulation of the differential cutting forces on the basis of the theory of oblique cutting. There are also known works describing the kinematics and dynamics of milling with the use of end mills with differently shaped cutting edges. Works [18, 19] present analytical models of cutting force as well as process stability tests for cylindrical and conical milling cutters with a wavy sinusoidal shape of a cutting edge. However, the results were not compared with other shapes of the cutting edge. Merdol and Altintas created a theoretical model for tools with the interrupted shape of a cutting edge. Dombovari proposed a model for predicting cutting forces using serrated tools. The article confirms the practical advantages of using this type of tools. Koca and Budak describe the simulation and optimization of cutter geometry [20]. Various parametric shapes of a cutting edge were tested in comparison with a continuous shape, for which the lowest cutting forces were obtained. In work [21] the influence of the depth of the cutting edge's profile on cutting forces was investigated. An analytical model was developed, and on its basis a simulation and experimental tests were conducted. The results proved that when increasing the depth of the cutting edge's profile, the cutting forces are decreasing. In his work, Campomanes proposed a dynamics and mechanics model of end mills with the interrupted shape of a cutting edge [22]. The model shows the average values of cutting force coefficients and approximate chip thickness. Moreover, Campomanes found that the introduction of the interrupted shape of a cutting edge improves process stability. Grabowski *et al*. presented a method of cutting forces prediction as well as examined the stability of indexable cutting tools [23]. Sultan and Okafor on the other hand developed a model for prediction of cutting forces for a bull-nose wavy-edge helical end mill [24]. They examined the influence of geometric parameters of WEBNHE on the resultant cutting force as well as on the predicted cutting force components. Budak and Techranizadeh studied the effect of serration and proposed a new method for optimizing serrated shapes [25].

However, these were only fragmentary studies, without a comparison with other types of the shape of a cutting edge. Therefore, there is a lack of works focusing on the influence of the shape of a cutting edge on the HPC process of aluminum alloys, and on the cutting forces and its variations in particular. Considering the above, comparative studies of high performance milling of a selected aluminum alloy AlZn5.5MgCu, commonly used in the aviation industry for hull structural parts and aircraft wings, were conducted. Four different shapes of a cutting edge of end mills dedicated to HPC machining of aluminum alloys were tested under the same conditions. Based on the recorded cutting force components values, mathematical models were developed, allowing a comparative assessment of the examined shapes of a cutting edge to be performed.

2. Materials and methods

The experimental tests were carried out on a DMG's DMU 100 MonoBlock multi-axis machining center. The machine tool was equipped with specialized measuring equipment dedicated to measuring cutting force components. The measurement of the cutting force components was carried out in the workpiece system. A cutting force measuring platform is an original design based on a four, three-component Kistler's piezoelectric sensors type 9601A31. They are characterized by a measuring range of ±2.5 kN in the direction of the X and Y axes and ±5 kN in the direction of the Z axis. In the milling table plane, $F_x(F_f)$ and $F_y(F_{fN})$ cutting force components were measured and in the direction of the Z axis, $F_z(F_a)$ was measured. The voltage signal from the dynamometer was transferred to the National Instruments' A/D converter type USB-6003. Force signals after conversion were recorded with the use of the Signal Express software. Fig. 2 presents the test stand.

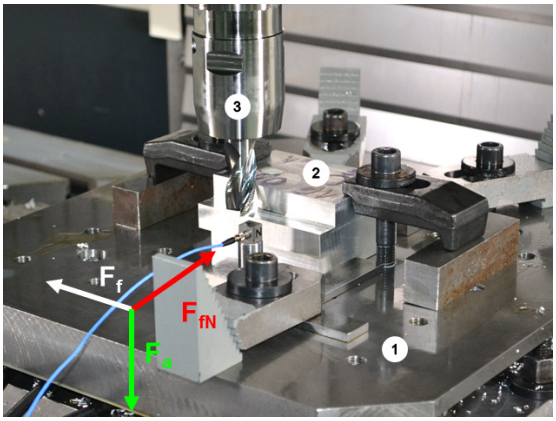

Fig. 2 Test stand: 1 – cutting force measuring platform, 2 – test sample, 3 – end mill

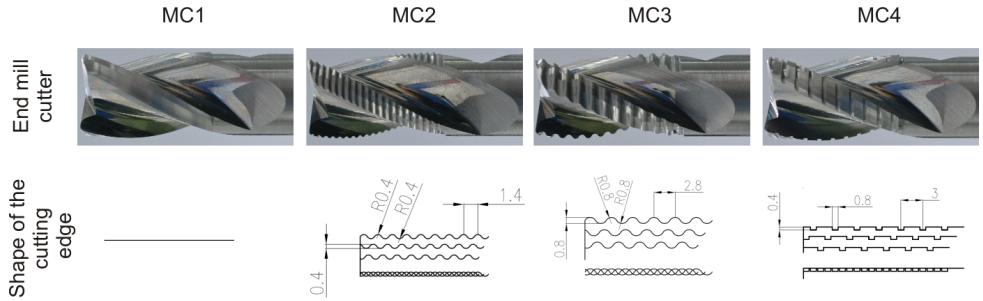

Fig. 3 The shape of a cutting edge

The test samples were made of AlZn5.5MgCu aluminum alloy. The experimental tests were carried out using 3 flute end mills made of carbide type DK 460UF, commonly used for cutting tools dedicated to machining aluminum alloys and recommended by Gühring. It is an ultra-fine cemented carbide with a grain size of about 0.5 μm and hardness of 1620 HV. The recommended cutting speed for this material was determined by the manufacturer and equaled v_c = 700 m/min. All the tools used in experimental tests had polished surfaces of the flutes, which minimized the possibility of the occurrence of the adhesive phenomena. Four end mills were used, each with a different shape of a cutting edge (Fig. 3). A continuous (notation MC1), sinusoidal wavy fine (MC2), sinusoidal wavy thick (MC3), and interrupted rectangular (MC4) shape of a cutting edge were used.

The milling tests were conducted with constant parameters of: axial depth of cut a_p and cutting speed v_c (Table 1). The value of the cutting speed v_c was a result of the carbide manufacturer's recommendations, whereas the value of the axial depth of cut was determined based on the modal analysis of the test stand system. A critical value of the axial depth of cut was determined a_{pkryt} = 15 mm, for which the system is always stable regardless of the spindle rotational speed. The variable cutting parameters were the radial depth of cut a_e and the feed per tooth f_z (Table 1). The experimental tests were carried out based on a three-level full design of experiment PS/DK 3n, modified taking three levels of values for a_e and f_z. As a result, for each tool, 9 experimental tests were carried out, while some tests were characterized by a constant cutting volume.

Table 1 Values of technological parameters

Parameter	Value
Rotational speed n, rpm	11000
Cutting speed v_c, m/min	690
Axial depth of cut a_p, mm	15
Radial depth of cut a_e, mm	8, 12, 16
Feed per tooth f_z, mm/tooth	0.075, 0.1, 0.15

3. Results and discussion

For each milling test, three cutting force components were recorded, and each component was analyzed separately. First milling tests were carried out with end mill with the continuous shape of a cutting edge. Such a shape of a cutting edge is commonly used in milling tools, and models of cutting force components for such geometry are well known. However, the experimental tests for the end mill with a continuous shape of a cutting edge were carried out in order to obtain reference values for the remaining geometries.

3.1 Analysis of the results

The analysis of the results of the tests carried out with the end mill with a continuous shape of a cutting edge indicates that all cutting force components change monotonically. Both in the case of feed per tooth f_z and the radial depth of cut a_e, the increase of cutting force component values in the feed, normal to feed and axial directions is observed. It was also noticed that a change in feed per tooth f_z at a constant radial depth of cut a_e results in a much higher increase in all the cutting force components (even up to about 50 %), than a change in a_e at a constant f_z (increase only up to about 20 %). The obtained values were adopted as reference for end mills with a modified shape of a cutting edge in order to present the effect of the shape of a cutting edge on cutting force values in relation to the conventional end mill. The relative change in force components was calculated from the equation:

$$\Delta_x = \frac{x - x_{ref}}{x_{ref}} \cdot 100\ \% \tag{1}$$

Where x is a current value of the analyzed cutting force component and x_{ref} is the respective value of the cutting force component for the end mill with a continuous shape of a cutting edge.

In order to present the influence of the cutting edge shape modification on the values of F_f force component, the results are presented graphically in the form of values calculated according to the Eq. 1 in relation to the continuous shape of a cutting edge. Analyzing the values of the feed cutting force component for various shapes of a cutting edge, significant differences can be observed in comparison with an end mill with a continuous shape of a cutting edge. Negative values mean a decrease in force compared to the standard end mill (Fig. 4).

The presented results can lead to a conclusion, that a modification of the shape of a cutting edge has a great impact on the values of the F_f cutting force component. Application of the wavy fine or wavy thick shape of a cutting edge can lead to a decrease in the F_f component from a dozen up to 35 %. In addition, the higher the cut layer cross-section, the higher the reduction in the F_f component value. However, using an interrupted rectangular shape of a cutting edge has a different impact on the F_f component values, depending on the cutting parameters. For radial depth of cut a_e = 8 mm, an increase in F_f values was observed in relation to MC1 end mill. However, for higher values of a_e, a significant reduction in the feed cutting force component was observed. For all the end mills, the highest decrease in feed force component was observed for higher values of a_e. It can be an effect of the increase in the arc of engagement as well as employing more cutting edges, which leads to a higher thickness of the cut layer.

The normal to feed cutting force component F_{fN} was then analyzed. The value of the normal to feed component is mainly responsible for the mechanical load on the workpiece's wall and its possible deformation. Moreover, it causes bending stresses in the tool. Thus, the goal is to minimize F_{fN} value. The recorded values of F_{fN} can lead to a conclusion, that using a wavy or interrupted shape of a cutting edge does not affect the force values in comparison with the continuous shape of a cutting edge. A monotonic increase of F_{fN} component along with the increase in feed per tooth f_z and radial depth of cut a_e was noted. It may also be observed, that a larger gradient of the normal to feed component increase occurs when changing feed per tooth f_z value. The research also shows that the use of a cutting shape modification results in a significant reduction in F_{fN} component for all pairs of technological parameters in comparison with the MC1 end mill. This is confirmed by the results of the F_{fN} component in relation to the values recorded when milling with the MC1 end mill (Fig. 5).

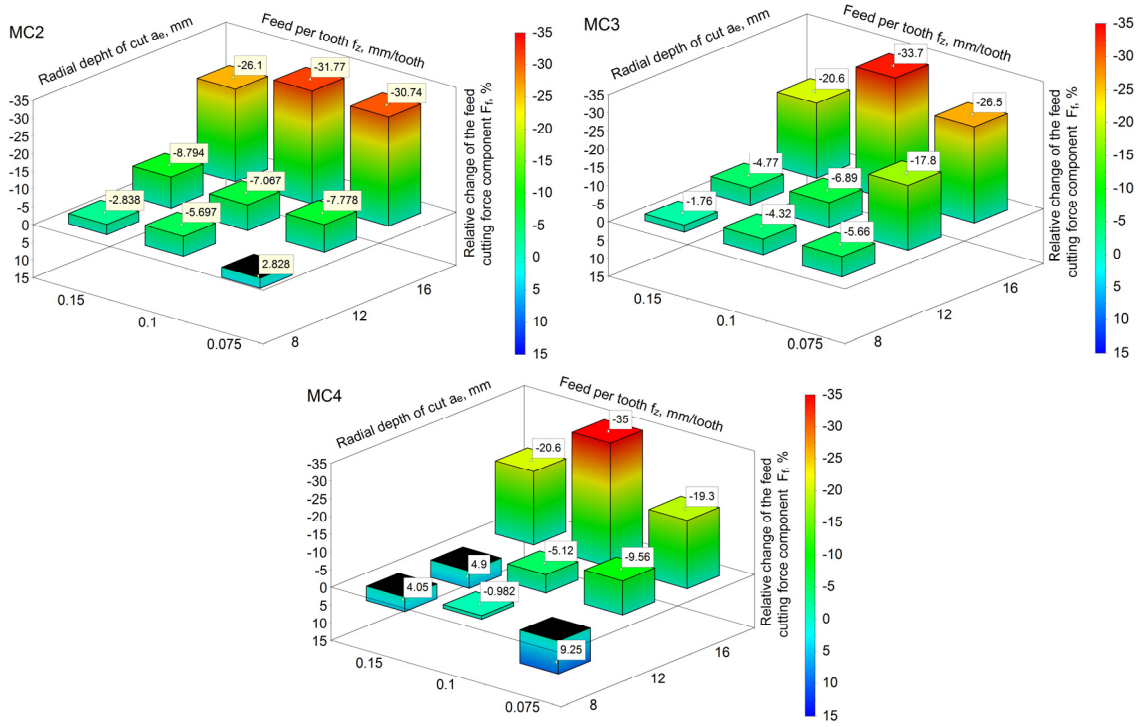

Fig. 4 Relative change of the feed cutting force component F_f for different shapes of a cutting edge in relation to the continuous shape

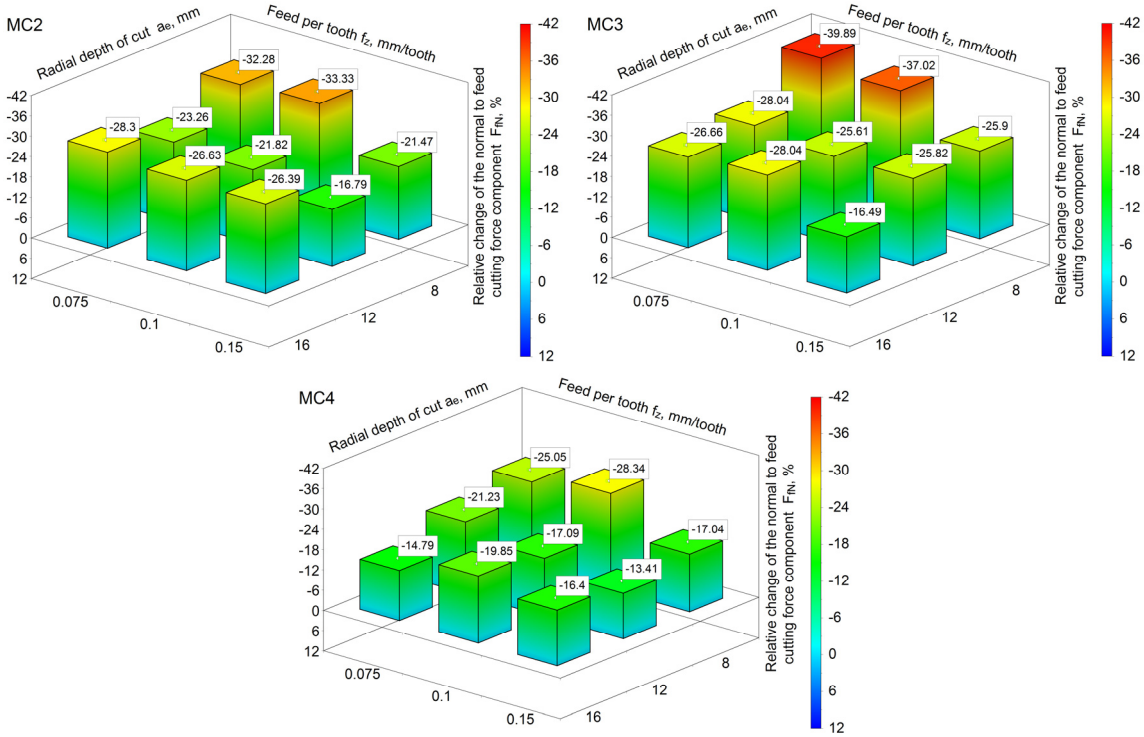

Fig. 5 Relative change of the normal to feed cutting force F_{fN} for different shapes of a cutting edge in relation to the continuous shape

Based on the conducted experimental tests, it can be noted that the highest reduction in normal to feed component F_{fN} was obtained for end mills with the wavy shape of a cutting edge, on average by 25 % in relation to the end mill with the continuous shape of a cutting edge. The highest reduction in normal to feed component F_{fN} was observed for cutting parameters a_e = 8

mm and f_z = 0.075 mm/tooth. For the end mill with a wavy thick shape of a cutting edge a 40 % decrease, and for the end mill with a wavy fine shape a 32 % decrease in normal to feed component were recorded in relation to the end mill with the continuous shape of a cutting edge. In the case of the interrupted shape of a cutting edge MC4, a reduction in normal to feed component of about 15 % was observed in relation to the end mill with the continuous shape of a cutting edge. Moreover, for the pairs of parameters a_e = 8 mm and f_z = 0.15 mm/tooth, a_e = 12 mm and f_z = 0.1 mm/tooth, a_e = 16 mm and f_z = 0.075 mm/tooth and while maintaining constant cutting volume Q_w = 594 cm^3/min it can be noted, that the relative change in normal to feed component F_{fN} value was at the same level for all tested shapes of a cutting edge.

The third measured and analyzed component of the cutting force was the axial component. In the case of milling, the component acts in the direction of a tool's axis and creates compressive stresses of the tool. Stiffness of a tool is much higher in the axial direction than in the radial direction, so even relatively high values of the F_a component do not lead to the loss of machining stability.

The recorded values of F_a prove that using end mills with the interrupted or wavy shape of a cutting edge leads to a reduction in axial cutting force component F_a, regardless of the f_z and a_e parameters. Moreover, changes in the F_a component are monotonic along with the increase in feed per tooth f_z and in the radial depth of cut a_e. Fig. 6 presents the changes of the axial force component in relation to the end mill with the continuous shape of a cutting edge.

The lowest values of the axial cutting force component were recorded for the end mill with the wavy thick shape of a cutting edge. The axial component was lower on average by about 18 % in relation to the end mill with the continuous shape of a cutting edge. The results obtained for the MC2 end mill also show a significant decrease in the axial component F_a, on average approx. 18 % for the radial depth a_e = 16 and 8 mm, while for a_e = 12 mm the recorded decrease was equal approx. 3 % in comparison with the end mill with the continuous shape of a cutting edge. In the case of MC4 end mill, the value of the axial cutting force component was reduced as well. The average relative value of the axial component F_a was about 12 % lower for the tested technological parameters in relation to the end mill with the continuous shape of a cutting edge.

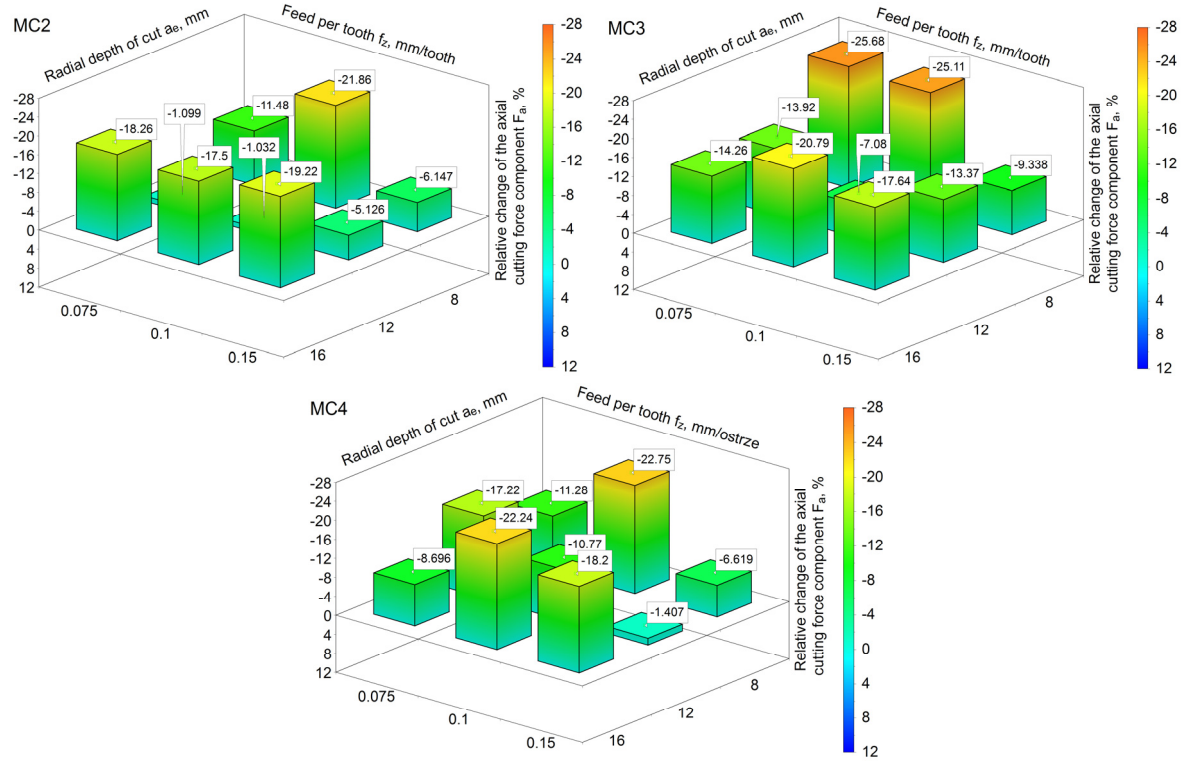

Fig. 6 Relative change of the axial cutting force component F_a for different shapes of a cutting edge in relation to the continuous shape

The comparative analyses indicate clearly that using a modifying shape of a cutting edge in end mills has a significant impact on the values of the cutting force components. Utilizing a non-continuous cutting edge results in the division of the cut layer and division of the chip. Moreover, the effective number of cutting edges is changed. In the case of the continuous shape of a cutting edge, the cutting edge is in contact with a workpiece along its entire length. In the case of MC2, MC3 and MC4 end mills, the cutting edge is in contact with a workpiece in several points. As the results and analyses show, the division of the machining allowance and non-continuous contact of the edge with a machined material in most cases has a positive influence on the machining process. In most cases, a significant reduction in cutting force components, mainly normal to feed component F_{fN}, was recorded. However, in order to be able to design the machining process and to determine the cutting force components values for any values of technological parameters, it is necessary to develop mathematical models of the cutting force components.

3.2 Modelling of the cutting force components

In order to develop mathematical models, statistical analyses of the obtained results were conducted. The analyses were performed in JMP 12 software employing response surface methodology (RSM). The general form of the response equation is in the form:

$$y = A + Bf_z + Ca_e + Df_z^2 + Ea_e^2 + Ff_z a_e \tag{2}$$

where A is constant coefficient, B and C are coefficients of main linear effects, D and E are coefficients of main square effects, and F is coefficient of the interaction effect.

Subsequently, the significance of obtained interactions between the technological parameters was analyzed. The boundary level of statistical significance of each parameter was set at 0.05. Table 2 presents the levels of statistical significance of the influence of each component of the equation on the value of the cutting force components.

Table 2 Levels of statistical significance of the equation's components

Type of a cutting edge	Cutting force component	Level of statistical significance				
		f_z	a_e	a_e^2	f_z^2	$f_z a_e$
MC1	F_f	0.00003	0.00083	0.15617	0.29825	0.55984
	F_{fN}	0.00001	0.00009	0.1624	0.4261	0.00836
	F_a	0	0.00133	0.93012	0.43903	0.01254
MC2	F_f	0.00001	0.94583	0.25446	0.69474	0.96378
	F_{fN}	0.00002	0.00049	0.00649	0.78576	0.28006
	F_a	0	0.0159	0.00649	0.73337	0.37894
MC3	F_f	0.00001	0.03621	0.35369	0.56736	0.95489
	F_{fN}	0.00002	0.00015	0.26887	0.58989	0.02321
	F_a	0	0.0002	0.00441	0.92783	0.72537
MC4	F_f	0.00001	0.88059	0.2982	0.25434	0.76364
	F_{fN}	0.00003	0.00051	0.10812	0.472	0.1691
	F_a	0.00001	0.22696	0.31983	0.43137	0.85631

Analyzing the obtained values of levels of statistical significance for the end mill with a continuous shape of a cutting edge, it can be noticed that the value of the feed cutting force component F_f is very much dependent on the feed per tooth f_z and on the radial depth of cut a_e. In the case of the normal to feed cutting force component F_{fN} as well as the axial component F_a, the forces were additionally influenced by the value of the product of the f_z and a_e parameters. Considering the remaining shapes of a cutting edge it can be observed, that for the interrupted shape of a cutting edge, the value of the feed cutting force component F_f depends mainly on the feed per tooth f_z, whereas the value of the normal to feed cutting force component F_{fN} and the axial cutting force component F_a, as in the case of the end mill with a continuous shape of a cutting

edge, depends on both the a_e and f_z parameters. When analyzing end mills with wavy shapes of a cutting edge, it can be concluded that the values of the cutting force components depend on both the a_e and f_z parameters.

By rejecting the components of the equation, for which the level of statistical significance was over 0.05, models of the cutting force components for each tested end mill were developed. The models of the cutting force components are presented in Table 3. For all of the developed relationships, the coefficient of determination R^2 above 0.9 was obtained, which indicates a very good fit of the models. Subsequently, the responses of the developed models for the full range of parameters f_z and a_e were determined. The results are presented in the following graphs.

All the developed models were tested in terms of statistical significance with the use of analysis of variance. The probability value for all the developed models was equal $p < 0.0001$. It means, that in each case the value of probability was lower than the assumed level of significance $\mu = 0.05$. Next, the assumptions of the analysis of variance with the normality of residuals were tested. The normality of residuals was checked using the Shapiro and Wilk's test. For all the developed models the analysis proved, that the residuals are normally distributed.

It can be observed that in the case of MC1 end mill, the model of the feed cutting force component F_f is completely different than models of the other end mills with the modified shape of the cutting edge (Fig. 7).

The obtained graph for the MC1 indicates the influence of the radial depth of cut a_e on the F_f component value. In the case of the remaining end mills, the F_f force depends exclusively on f_z. The difference in the F_f component value of almost 200 N in favor of the MC2, MC3 and MC4 end mills is also noteworthy. These differences result mainly from the division of the machining allowance due to the division of the cutting edge with a wavy or interrupted profile. This results in a decrease in the F_f component and in a change of the model.

A comparison between the graphical representations of the normal to feed component F_{fN} models shows different relationships than in the case of the F_f component (Fig. 8). It is evident, that adopting a modification in the shape of a cutting edge leads to a significant reduction in the F_f component that equals for the maximum values of a_e and f_z up to 400 N. However, a change in the shape of a cutting edge does not affect the F_{fN} component's model uniformly.

It turns out, that for MC3 and MC4 end mills the functions are not the same as for the end mill with the continuous shape of a cutting edge. Only the MC2 end mill is characterized by a different form of the F_{fN} component's model. The obtained surface is clearly curved, which means a nonlinear and higher impact of mainly radial depth of cut a_e on the F_{fN} value. This may be explained by the very fine division of the cutting edge which results in high chip defragmentation. As a result, for low values of a_e and f_z, the value of the F_{fN} component is much higher than for MC3 and MC4 end mills. This, in turn, means that the MC2 end mill is mostly dedicated to milling with large cut layer cross-sections.

Table 3 Models of the cutting force components

End mill	Models of the cutting force components	R^2
MC1	$F_f = -202.59 + 4848.57f_z + 26a_e$	0.96
	$F_{fN} = -66 + 9240f_z + 50a_e + 586.71(f_z - 0.108)(a_e - 12)$	0.99
	$F_a = -58.95 + 5652.38f_z + 15.62a_e + 295.71(f_z - 0.108)(a_e - 12)$	0.99
MC2	$F_f = 80.43 + 4251.42f_z$	0.98
	$F_{fN} = -112.42 + 8296.19f_z + 38.75a_e + 9.39(a_e - 12)(a_e - 12)$	0.98
	$F_a = 71.53 + 5098.09f_z + 7.85a_e - 5.88(a_e - 12)(a_e - 12)$	0.99
MC3	$F_f = -28.11 + 4905.71f_z + 3.41a_e$	0.99
	$F_{fN} = -496.33 + 8713.33f_z + 56.04a_e + 561.07(f_z - 0.108)(a_e - 12)$	0.98
	$F_a = 72.43 + 5200.95f_z + 13.58a_e - 2.97(a_e - 12)(a_e - 12)$	0.99
MC4	$F_f = 36.85 + 4956.19f_z$	0.96
	$F_{fN} = -303.357 + 8670.47f_z + 51.12a_e$	0.96
	$F_a = 45.54 + 5532.38f_z$	0.90

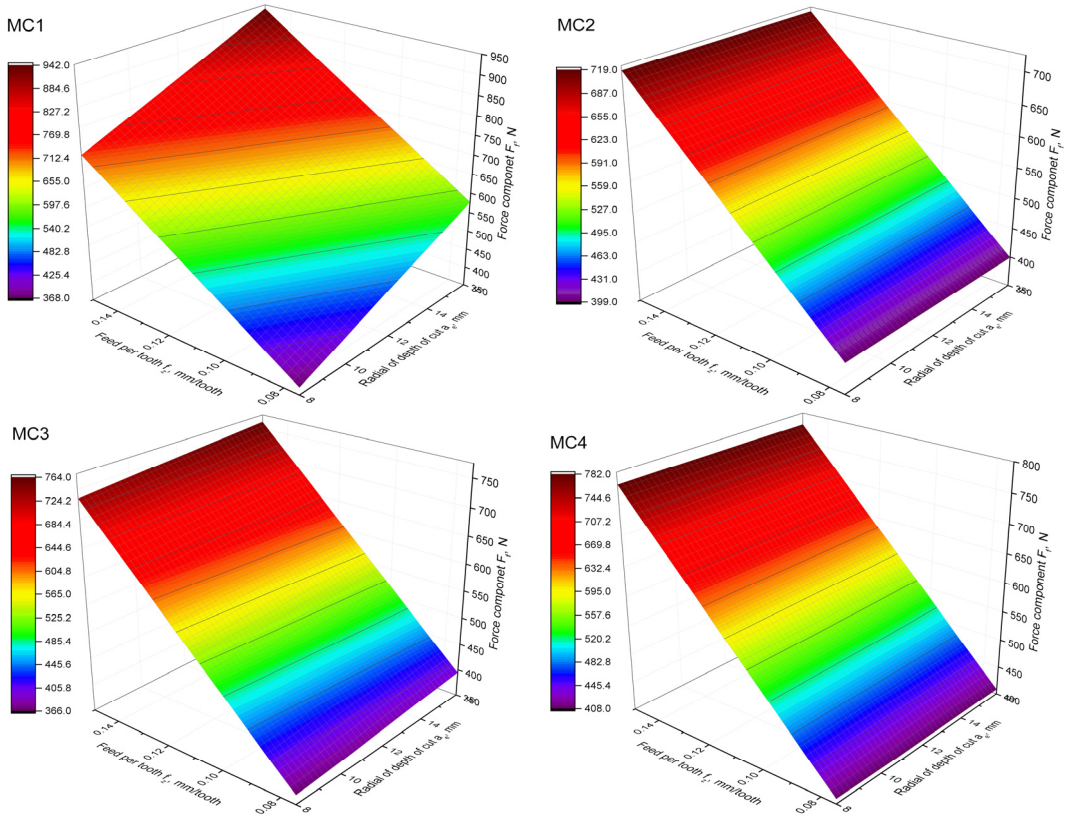

Fig. 7 Graphical representation of the feed cutting force component F_f models

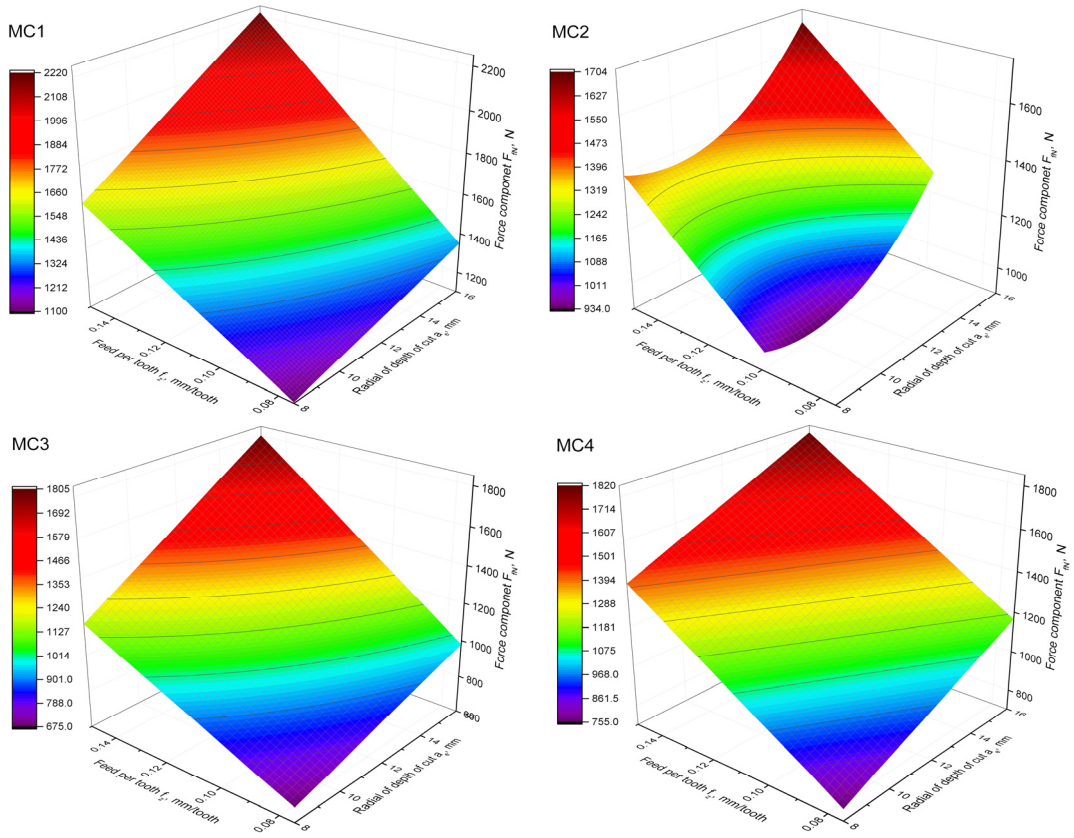

Fig. 8 Graphical representation of the feed cutting force component F_{fN} models

The analysis of graphical representations of the axial component F_a models allows to observe, that only in the case of the MC4 end mill a function independent of the radial depth of cut a_e was obtained (Fig. 9). In the case of other end mills, the value of the F_a component also depends on the radial depth of cut, the strongest for MC2 and MC3 end mills. Moreover, for wavy shapes of a cutting edge, the obtained surface is clearly curved which indicates a nonlinear influence of mainly a_e parameter on the force value. The highest influence was noted for the average values of the radial depth of cut. The value of the F_a component is noteworthy as well, and it is the lowest for the MC4 end mill. It is the result of the fact that only a modification of the cutting edge shape in the rectangular form leads to a significant decrease in the axial cutting force component F_a.

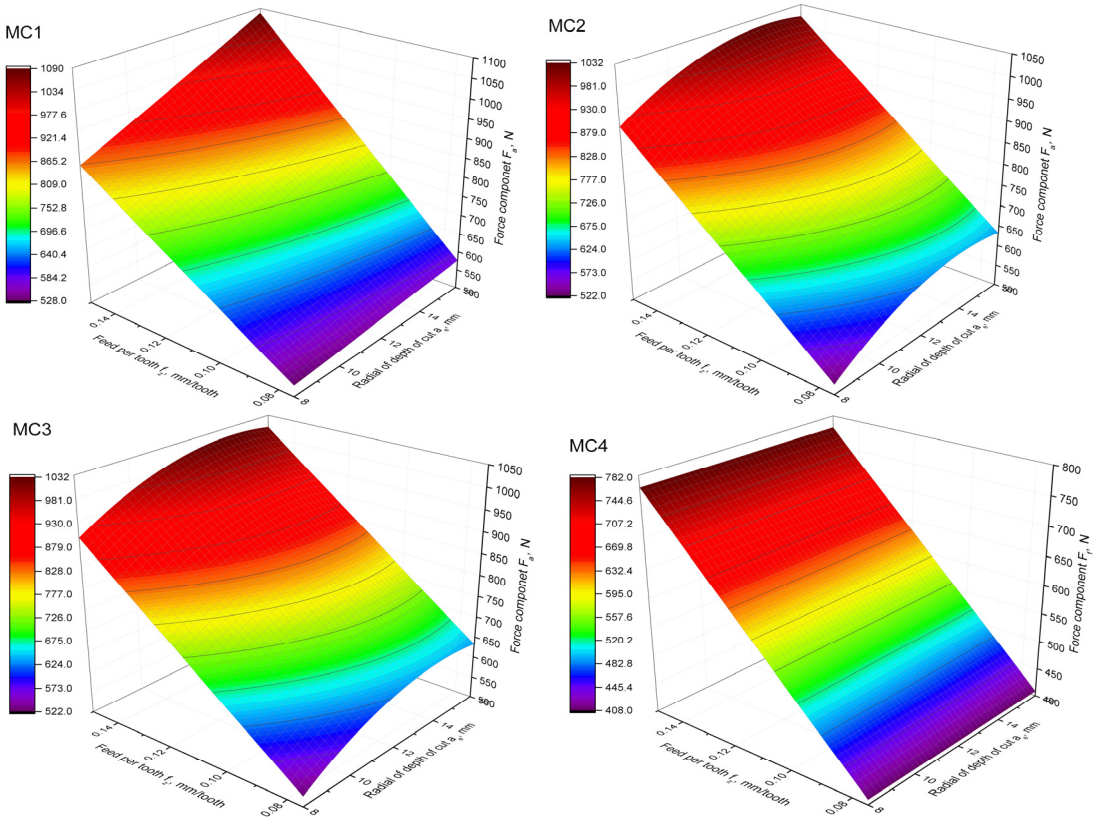

Fig. 9 Graphical representation of the axial cutting force component F_a models

4. Conclusion

In order to reduce the time and cost of manufacturing, high performance milling becomes an increasingly popular method of machining. End mills with the interrupted or wavy shape of a cutting edge are dedicated to this type of machining. Due to the variety of cutting edge shape modifications, experimental tests of the influence of the shape of a cutting edge on the cutting force components for three types of shapes (wavy fine, wavy thick and interrupted rectangular) were conducted. Analyzes of the results of the experiment were carried out by comparing them to the end mill with a continuous shape of a cutting edge as a reference tool.

It was observed, that modifying the shape of a cutting edge has a significant impact on the F_f cutting force component, adopting the wavy fine or wavy thick shape of a cutting edge leads to the decrease in F_f component from a dozen up to even 35 %. Moreover, it was determined, that a change in the shape of a cutting edge results in a decrease in the normal to feed cutting force component F_{fN}, the highest for end mills with wavy shapes of a cutting edge, on average 25 % in comparison with the end mill with the continuous shape of a cutting edge. Modifying the shape of a cutting edge leads to a decrease in the axial cutting force component F_a regardless of f_z and a_e parameters. The highest decrease of the axial component, of approx. 18 % in comparison with

the end mill with a continuous shape of a cutting edge, was obtained for the end mill with a wavy thick shape of a cutting edge.

Adopting a modified shape of a cutting edge makes the F_f component dependent only on the f_z parameter, whereas in the case of the continuous shape of a cutting edge, the F_f component depends on both a_e and f_z parameters. In the case of the end mill with a wavy fine shape of a cutting edge, a different form of the F_{fN} component model was obtained than in the case of other end mills. Radial depth of cut a_e exhibits a non-linear influence on the F_{fN} value. Moreover, adopting an interrupted rectangular shape of a cutting edge leads to the lack of influence of radial depth of cut a_e on the value of the axial component F_a.

The obtained test results allow to formulate a few practical conclusions and advises for users of end mills with serrated cutting edges. Using end mills with serrated cutting edges allows to significantly reduce the values of the cutting force components. Thus, it is possible to increase cutting parameters compared to the machining when using cutters with a continuous shape of a cutting edge. As a result, using end mills with serrated cutting edges, one may achieve higher milling efficiency. Another practical conclusion resulting from the developed cutting force components' models is the lack of influence of radial depth of cut a_e on the value of the feed cutting force component F_f for end mills with serrated cutting edges. It follows that in practice using end mills with serrated cutting edges, higher values of radial depth of cut a_e can be used in comparison with the conventional cutters. Higher a_e values allow to increase machining efficiency without the risk of increasing the tool's load in the feed direction.

The test results confirm, that end mills with serrated cutting edges should be used in high performance machining, where high values of f_z and a_e occur. In addition, such end mills could potentially be applied to machining enclosed spaces, pockets or thin-walled structural elements. Lower values of the cutting force components in feed and normal to feed directions result in lower tool's deflection and lower deflection of milled thin walls. Thanks to this advantage, using end mills with serrated cutting edges helps to increase machining efficiency and at the same time allows to achieve the higher shape and dimensional accuracy of thin-walled parts.

In future works, authors plan to analyze surface roughness obtained after milling with end mills with serrated cutting edges. Despite the fact, that such cutters are dedicated to rough machining, surface topography after rough machining influences the finishing process. In addition authors plan to conduct experimental and modelling tests concerning different shapes of a cutting edge, with a focus on the analysis of the influence of the wavy and interrupted shape pitch on the high performance milling of aluminum alloys.

References

[1] Burek, J., Zylka, L., Plodzien, M., Gdula, M., Sulkowicz, P. (2018). The influence of the cutting edge shape on high performance cutting, *Aircraft Engineering and Aerospace Technology*, Vol. 90, No. 1, 134-145, doi: 10.1108/AEAT-11-2015-0243.

[2] Budak, E. (2006). Analytical models for high performance milling. Part I: Cutting forces, structural deformations and tolerance integrity, *International Journal of Machine Tools and Manufacture*, Vol. 46, No. 12-13, 1478-1488, doi: 10.1016/j.ijmachtools.2005.09.009.

[3] Masood, I., Jahanzaib, M., Haider, A. (2016). Tool wear and cost evaluation of face milling grade 5 titanium alloy for sustainable machining, *Advances in Production Engineering & Management*, Vol. 11, No. 3, 239-250, doi: 10.14743/apem2016.3.224.

[4] Santos, M.C., Machado, A.R., Sales, W.F., Barrozo, M.A.S., Ezugwu, E.O. (2016). Machining of aluminum alloys: A review, *The International Journal of Advanced Manufacturing Technology*, Vol. 86, No. 9-12, 3067-3080, doi: 10.1007/s00170-016-8431-9.

[5] Tang, A., Liu, Z. (2008). Deformations of thin-walled plate due to static end milling force, *Journal of Materials Processing Technology*, Vol. 206, No. 1-3, 345-351, doi: 10.1016/j.jmatprotec.2007.12.089.

[6] Ren, S., Long, X., Meng, G. (2018). Dynamics and stability of milling thin walled pocket structure, *Journal of Sound and Vibration*, Vol. 429, 325-347, doi: 10.1016/j.jsv.2018.05.028.

[7] Borojević, S., Lukić, D., Milosević, M., Vukman, J., Kramar, D. (2018). Optimization of process parameters for machining of Al 7075 thin-walled structures, *Advances in Production Engineering & Management*, Vol. 13, No. 2, 125-135, doi: 10.14743/apem2018.2.278.

[8] Burek, J., Żyłka, Ł., Płodzień, M., Sułkowicz, P., Buk, J. (2017). The effect of the cutting edge helix angle of the cutter on the process of chips removing from the cutting zone, *Mechanik*, Vol. 11, 962-964, doi: 10.17814/mechanik.2017.11.152.

[9] Kuczmaszewski, J., Pieśko, P., Zawada-Michałowska, M. (2017). Influence of milling strategies of thin-walled elements on effectiveness of their manufacturing, *Procedia Engineering*, Vol. 182, 381-386, doi: 10.1016/j.proeng.2017.03.117.
[10] Shamsuddin, K.A., Ab-Kadir, A.R., Osman, M.H., (2013). A comparison of milling cutting path strategies for thin-walled aluminium alloys fabrication, *The International Journal of Engineering & Science*, Vol. 2, No. 3, 1-8.
[11] Guo, Y., Lin, B., Wang, W. (2019). Modeling of cutting forces with a serrated end mill, *Mathematical Problems in Engineering*, Vol. 2019, Article ID 1796926, doi: 10.1155/2019/1796926.
[12] Tsai, M.Y., Chang, S.Y., Hung, J.P., Wang, C.C. (2016). Investigation of milling cutting forces and cutting coefficient for aluminum 6060-T6, *Computers & Electrical Engineering*, Vol. 51, 320-330, doi: 10.1016/j.compeleceng.2015.09.016.
[13] Kaneko, K., Nishida, I., Sato, R., Shirase, K. (2018). Virtual milling force monitoring method based on in-process milling force prediction model to eliminate predetermination of cutting coefficients, *Procedia CIRP*, Vol. 77, 22-25, doi: 10.1016/j.procir.2018.08.196.
[14] Karpuschewski, B., Kundrák, J., Varga, G., Deszpoth, I., Borysenko, D. (2018). Determination of specific cutting force components and exponents when applying high feed rates, *Procedia CIRP*, Vol. 77, 30-33, doi: 10.1016/j.procir.2018.08.199.
[15] Li, D., Cao, H., Zhang, X., Chen, X., Yan, R. (2019). Model predictive control based active chatter control in milling process, *Mechanical Systems and Signal Processing*, Vol. 128, 266-281, doi: 10.1016/j.ymssp.2019.03.047.
[16] Yang, Y., Li, M., Li, K.R. (2014). Comparison and analysis of main effect elements of machining distortion for aluminum alloy and titanium alloy aircraft monolithic component, *The International Journal of Advanced Manufacturing Technology*, Vol. 70, No. 9-12, 1803-1811, doi: 10.1007/s00170-013-5431-x.
[17] Liu, X.-W., Cheng, K., Webb, D., Luo, X.-C. (2002). Improved dynamic cutting force model in peripheral milling. Part I: Theoretical model and simulation, *The International Journal of Advanced Manufacturing Technology,* Vol. 20, No. 9, 631-638, doi: 10.1007/s001700200200.
[18] Dombovari, Z., Altintas, Y., Stepan, G. (2010). The effect of serration on mechanics and stability of milling cutters, *International Journal of Machine Tools and Manufacture*, Vol. 50, No. 6, 511-520, doi: 10.1016/j.ijmachtools.2010.03.006.
[19] Merdol, S.D., Altintas, Y. (2004). Mechanics and dynamics of serrated cylindrical and tapered end mills, *Journal of Manufacturing Science and Engineering*, Vol. 126, No. 2, 317-326, doi: 10.1115/1.1644552.
[20] Koca, R., Budak, E. (2013). Optimization of serrated end mills for reduced cutting energy and higher stability, *Procedia CIRP*, Vol. 8, 570-575, doi: 10.1016/j.procir.2013.06.152.
[21] Rekers, S., Auerbach, T., Veselovac, D., Klocke, F. (2015). Cutting force reduction in the milling of aluminum alloys with serrated cutting tool edges, *Journal of Machine Engineering*, Vol. 15, No. 4, 27-36.
[22] Campomanes, M.L. (2002). Kinematics and dynamics of milling with roughing end mills, In: Dudzinski, D., Molinari, A., Schulz, H. (eds), *Metal Cutting and High Speed Machining*, Kluwer Academic Publishers Plenum Press, New York, USA, 129-140.
[23] Grabowski, R., Denkena, B., Köhler, J. (2014). Prediction of process forces and stability of end mills with complex geometries, *Procedia CIRP*, Vol. 14, 119-124, doi: 10.1016/j.procir.2014.03.101.
[24] Sultan, A.A., Okafor, A.C. (2016). Effects of geometric parameters of wavy-edge bull-nose helical end-mill on cutting force prediction in end-milling of Inconel 718 under MQL cooling strategy, *Journal of Manufacturing Processes*, Vol. 23, 102-114, doi: 10.1016/j.jmapro.2016.05.015.
[25] Tehranizadeh, F., Budak, E. (2017). Design of serrated end mills for improved productivity, *Procedia CIRP*, Vol. 58, 493-498, doi: 10.1016/j.procir.2017.03.256.